Electronic Supplementary Material (ESI) for New Journal of Chemistry.
This journal is © The Royal Society of Chemistry and the Centre National de la Recherche Scientifique 2021

Supporting Information

Pt Modified Ni-Mo-based Hydrate as Bifunctional Electrocatalysts for Overall Water Splitting

Yayu Guan[a,b] and Yuyu Liu,*[,a]

[a] Institute for Sustainable Energy, College of Sciences, Shanghai University, Shanghai 200444, China.

[b] Department of Physics, College of Sciences, Shanghai University, Shanghai 200444, China.

EXPERIMENTAL SECTION

1. Chemicals and materials

All chemicals, including nickel chloride ($NiCl_2$, 99.0%), sodium molybdate ($Na_2MoO_4 \cdot 2H_2O$, 99.0%), chloroplatinic acid hexahydrate ($H_2PtCl_6 \cdot 6H_2O$, 99.9%, Pt:37.5%+) were purchased from Shanghai TITAN Technology Co., Ltd and used without further treatments. Ruthenium oxide (RuO_2) and isopropanol were obtained from Aladdin Industrial Inc. Pt/C (20%) was provided by Shanghai Macklin Biochemical Co. Ltd.

2. Synthesis of materials

In order to remove the organic impurities and oxide layer, NF was ultrasonic cleaned by acetone, hydrochloric acid and ethanol separately, then dried at 60 ºC. The 1mmol nickel chloride and 1mmol sodium molybdate were completely dissolved in 35 ml Deionized (DI) water and transferred into the Teflon-lined stainless autoclave. The cleaned NF was treated in solution for 6 hours at 150 ºC to get precursor. The as-fabricated precursor was immersed in different Pt concentrations (0.015/0.03/0.06 mg mL^{-1}) of chloroplatinic acid solution for 1 hour, and then annealed in argon atmosphere at 200 ºC for 2 hours with heating rate of 5 ºC min^{-1} to obtain platinum modified nickel molybdenum hydrate catalysts. According to the different contents of Pt, they are defined as Ni-Mo@Pt-0.015, Ni-Mo@Pt-0.03, and Ni-Mo@Pt-0.06. The annealed sample without doping is defined as Ni-Mo.

In order to explore the difference between direct hydrothermal method and immersion method for modification of the Pt, more work has been done. First, 1mmol $NiCl_2$ and 1mmol $Na_2MoO_4 \cdot 2H_2O$ were dissolved in 35 ml of $H_2PtCl_6 \cdot 6H_2O$ solution with 0.03 mg mL^{-1} Pt to form a mixed solution. Then the solution was poured into a Teflon-lined stainless autoclave and the treated NF was putted into the solution. The autoclave was sealed and heated at 150 ºC for 6 hours in an electric oven. The final product was obtained after annealing in argon at 200 ºC for 2 hours and was defined as Ni-Mo-Pt-0.03.

3. Characterizations

The microstructure and structure characteristics of the hybrid materials were observed and analyzed by scanning electron microscopy (SEM) and transition electron microscopy (TEM). The valence state and phase composition of the elements were collected by X-ray photoelectron spectroscopy (XPS) and X-ray diffractometer (XRD).

4. Electrochemical measurements

Electrochemical catalytic measurements were performed in 1.0 M KOH aqueous electrolyte through a typical three-electrode cell system on CHI760E electrochemical workstation at room temperature. The as-fabricated samples were employed directly as the working electrode with the geometric area of 1 cm^2. Pt plate and Hg/HgO electrode (MMO) were used as counter and reference electrode, respectively. To prepare the Pt/C and RuO_2 electrodes (for performance comparison), catalyst (5 mg) and 20 μL of 5% Nafion solution were dispersed in 180 μL of isopropanol to form a homogeneous mixture. Then the catalyst ink was loaded onto a 1 cm^2 NF with a catalyst loading of 2.5-3 mg cm^{-2}. Linear sweep voltammetry (LSV) was recorded at a scan rate of 2 mV s^{-1}.

All potentials are obtained versus reversible hydrogen electrode (RHE) by converting the potentials based on the following equation

$$E_{(RHE)} = E_{(MMO)} + 0.098 + 0.059pH$$

All LSV curves were corrected with IR compensation with 90%. To investigate the long-term stability of Ni-Mo@Pt-0.03 catalyst, the amperometric i-t curve test was recorded at a definite constant current density.

Electrochemical double-layer capacitances (C_{dl}) have a linear relationship with effective active surface area. The C_{dl} values of samples were estimated by cyclic voltammetry (CV) tests with different scan rates of 20, 40, 60, 80,100 and 120 mV s^{-1}. The specific value was obtained by drawing Δj (j_a - j_c) as the ordinate and the scan rates as the abscissa, where the slope is equal to the double C_{dl}. In detail, j_a and j_c are the anodic and cathodic current densities, respectively.

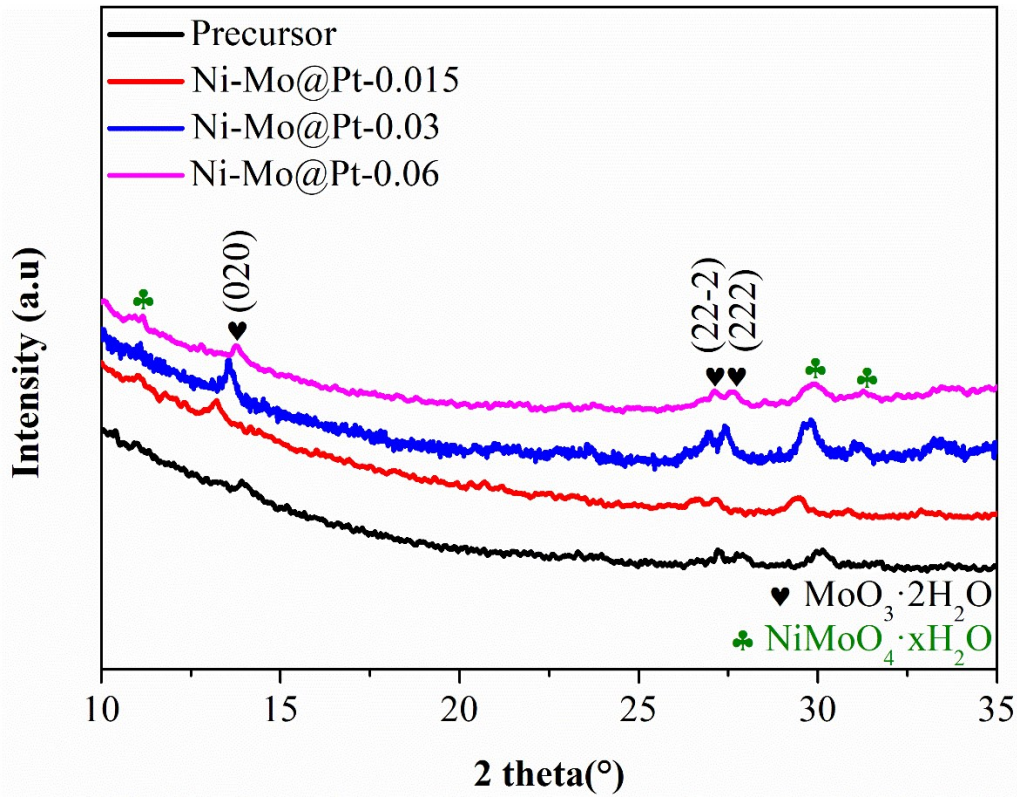

Fig. S1 Partial enlargement of XRD patterns of as-synthesized samples.

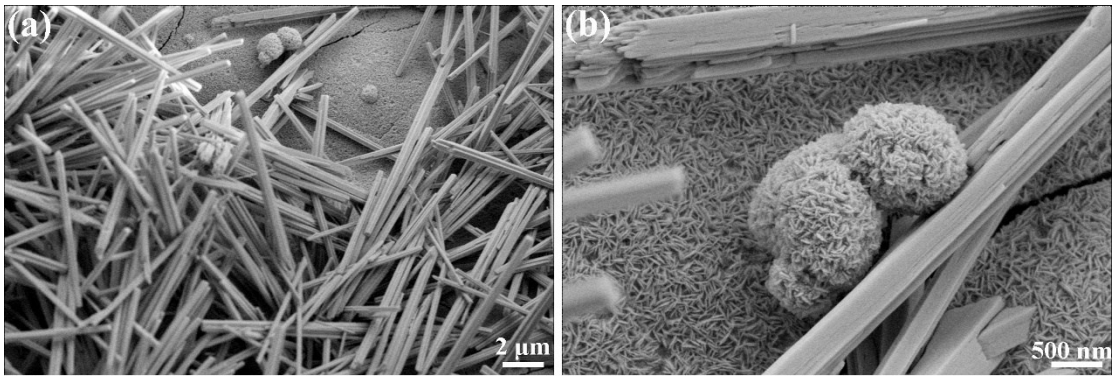

Fig. S2 SEM images of (a, b) precursor.

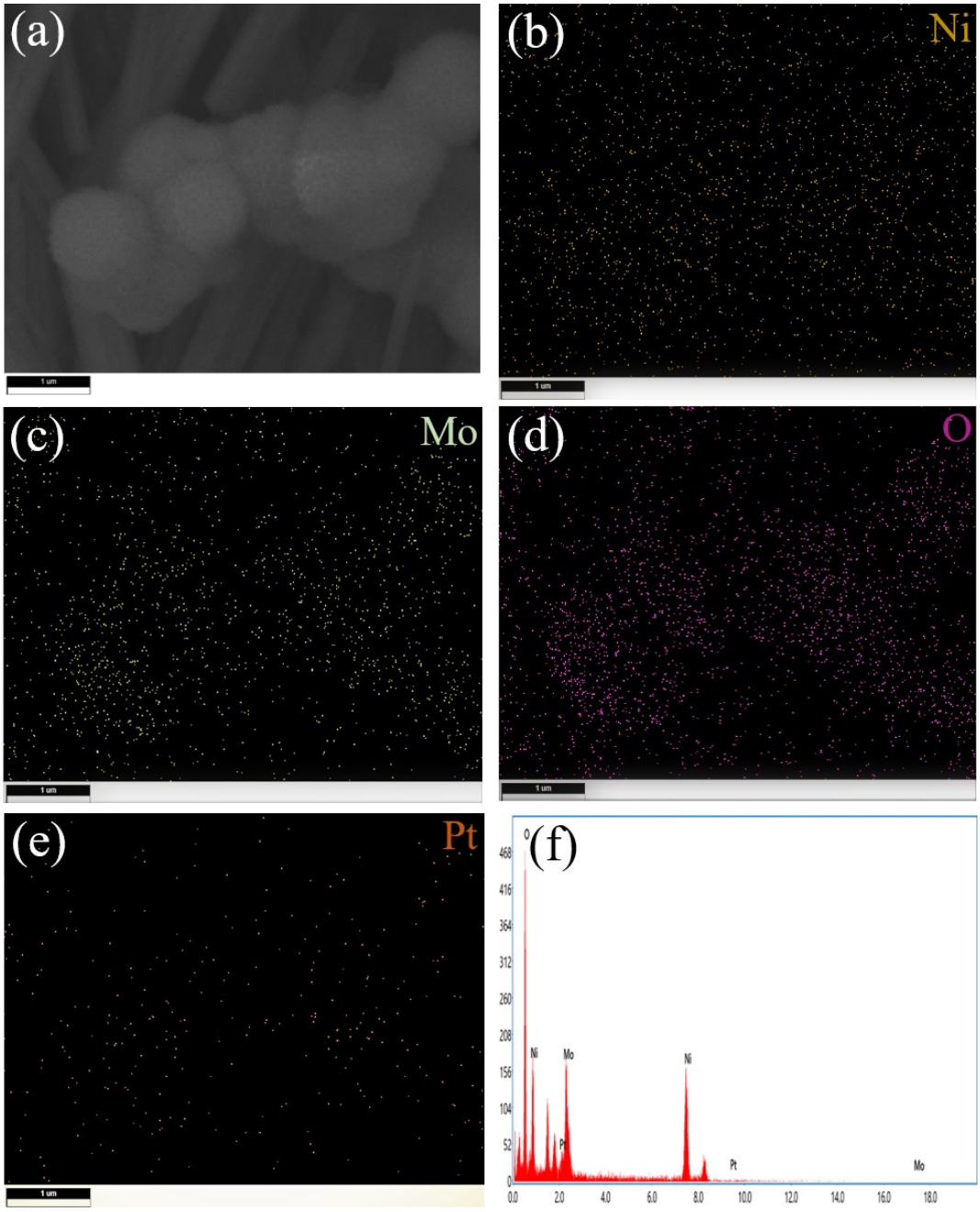

Fig. S3 EDS elemental mapping of Ni-Mo@Pt-0.03.

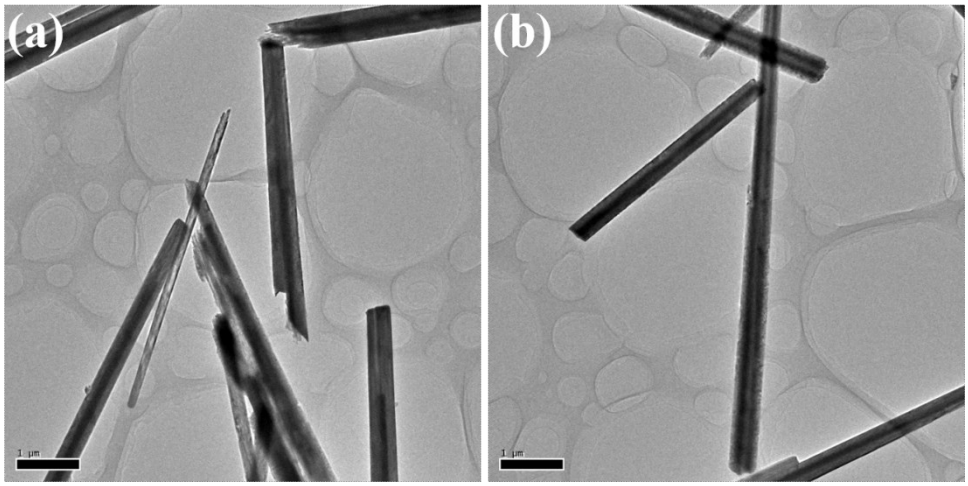

Fig. S4 TEM images of Ni-Mo@Pt-0.03.

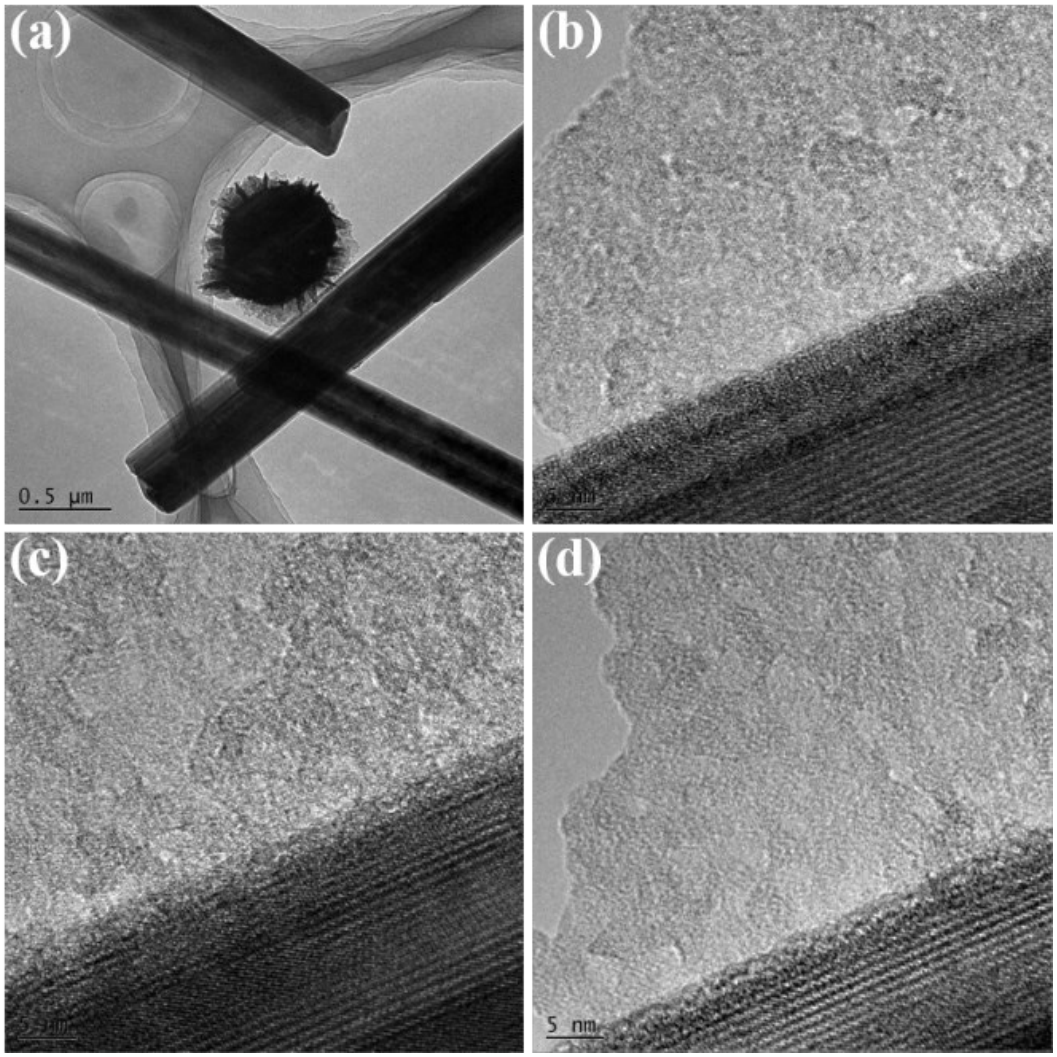

Fig. S5 TEM images of Ni-Mo.

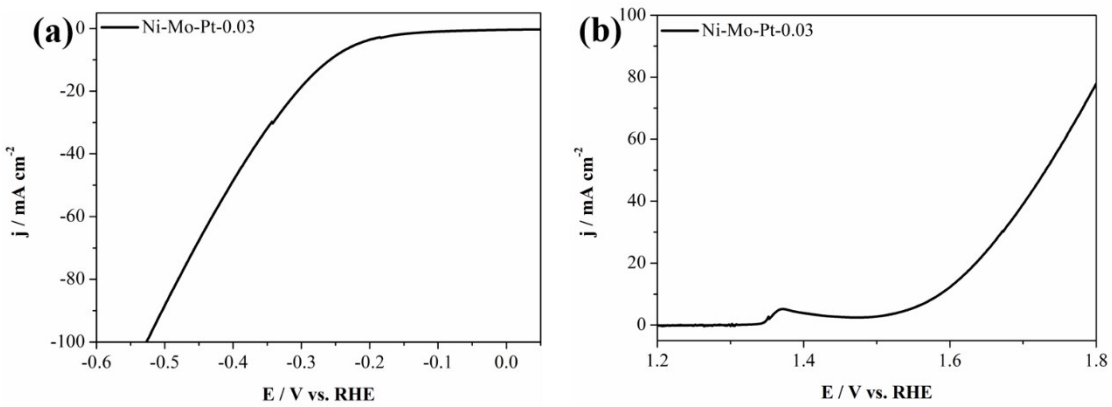

Fig. S6 Polarization curves of Ni-Mo-Pt-0.03: (a) HER; (b) OER.

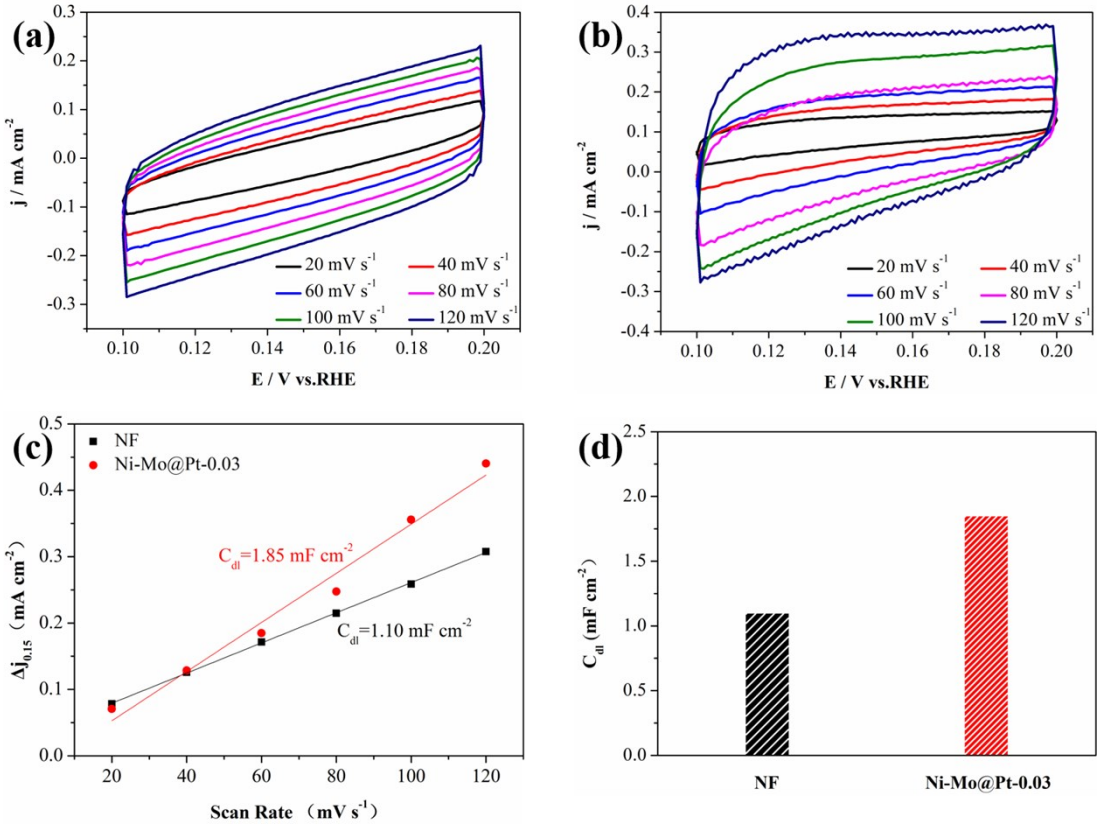

Fig. S7 Cyclic voltammograms (0.1-0.2 V vs. RHE) recorded at different scanning rate (20-120 mV s^{-1}) in 1.0 M KOH for (a) NF and (b) Ni-Mo@Pt-0.03. (c) The relationship of the as-synthesized catalysts between current density variation ($\Delta j_{0.15}=j_a-j_c$) and scan rate fitted to a linear regression allows for estimation of C_{dl}. (d) The values of C_{dl} are clearly displayed in the histogram.

Table. S1 Comparison of HER performance for Ni-Mo@Pt-0.03 with other recently reported HER catalysts in 1 M KOH.

Catalyst	Tafel slope (mV dec^{-1})	Current density (j, mA cm^{-2})	η at the corresponding j (mV)	Ref.
$Ni/Ni_{0.2}Mo_{0.8}N/MoO_3$	17	10	103	[1]
Cu@CoFe	36.4	10	171	[2]
NiCo-300	82.7	10	156	[3]
NiCo/CNF	-	10	220	[4]
$NiCo_2S_4$@NiFe LDH	101.1	10	200	[5]
$MoS_2/NiS\text{-}Ni_3S_2$	70.0	10	105	[6]
Co/Mo_2C@NC-800	166.85	10	121	[7]
R-Fe-Ni_2P	37.7	10	106	[8]
CoP@FeCoP	56.34	10	141	[9]
Ni-Mo@Pt-0.03	102.9	10	102	This work

Table. S2 Comparison of OER performance for Ni-Mo@Pt-0.03 with other recently reported OER catalysts in 1 M KOH.

Catalyst	Tafel slope (mV dec^{-1})	Current density (j, mA cm^{-2})	η at the corresponding j (mV)	Ref.
Co_3O_4 NPs	77	10	349	[10]
$Ni_{66}Fe_{34}$-NC	-	10	467	[11]
C@SnS_2/SnS	63	10	380	[12]
NiCoMn-LDHs	87	50	340	[13]
Fe_2Cu_5Ni	50	≈160	770	[14]
Mn/ZIF-67C(E)	80.99	10	338	[15]
$NiMnO_3$	141	50	>400	[16]
$NiCo_2O_4$@CoS/NF	92	30	359	[17]
$Ni(OH)_2$@CoB	94	100	460	[18]
Ni-Mo@Pt-0.03	145.3	50	399	This work

Table. S3 Comparison of the overall water splitting for Ni-Mo@Pt-0.03 with other bifunctional electrocatalysts in 1.0 M KOH.

Catalyst	Current density (j, mA cm^{-2})	Voltage (V)	Ref.
Co/NiLDH@ZIF-67	10	1.59	[19]
Co/Mo_2C@NC-800	10	1.67	[7]
ECT-NiMo/$NiMoO_4$	10	1.60	[20]
Al-Ni_3S_2/NF	10	1.58	[21]
CoP@FeCoP	10	1.68	[9]
$Fe_{0.9}Co_{0.05}S_{1.05}$	10	1.69	[22]
$NiCo_2Se_4$	10	1.58	[23]
CoVP@CC	10	1.61	[24]
$CoNi_2S_4$/Ni_3S_2@NF	10	1.65	[25]
Ni-Mo@Pt-0.03	10	1.58	This work

REFERENCES

1. R.Q. Li, S. Li, M. Lu, Y. Shi, K. Qu and Y. Zhu, J. Colloid Interface Sci., 2020, **571**, 48-54.
2. L. Yu, H. Zhou, J. Sun, F. Qin, D. Luo, L. Xie, F. Yu, J. Bao, Y. Li, Y. Yu, S. Chen and Z. Ren, Nano Energy, 2017, **41**, 327-336.
3. B. Zhang, X. Zhang, Y. Wei, L. Xia, C. Pi, H. Song, Y. Zheng, B. Gao, J. Fu and P.K. Chu, J. Alloys Compd., 2019, **797**, 1216-1223.
4. T.T. Gebremariam, F. Chen, Y. Jin, Q. Wang, J. Wang and J. Wang, Catal. Sci. Technol., 2019, **9**, 2532-2542.
5. J. Liu, J. Wang, B. Zhang, Y. Ruan, L. Lv, X. Ji, K. Xu, L. Miao and J. Jiang, ACS Appl. Mater. Interfaces, 2017, **9**,15364-15372.
6. Y. Guan, H. Xuan, H. Li and P. Han, Electrochim. Acta, 2019, **320**, 134614.
7. G. Liu, K. Wang, L. Wang, B. Wang, Z. Lin, X. Chen, Y. Hua, W. Zhu, H. Li and J. Xia, J. Colloid Interface Sci.,2021, **583**, 614-625.
8. M. Li, J. Wang, X. Guo, J. Li, Y. Huang, S. Geng, Y. Yu, Y. Liu and W. Yang, Appl. Sur. Sci., 2021, **536**, 147909.
9. J. Shi, F. Qiu, W. Yuan, M. Guo and Z.-H. Lu, Chem. Eng. J., 2021, **403,** 126312.
10. A.G. Abd-Elrahim and D.-M. Chun, J. Alloys Compd., 2021, **853**, 156946.
11. M. Ma, A. Kumar, D. Wang, Y. Wang, Y. Jia, Y. Zhang, G. Zhang, Z. Yan and X. Sun, Appl. Catal. B-Environ., 2020, **274**, 119091.
12. M. Jiang, T. Han and X. Zhang, J. Colloid Interface Sci. 2021, **583**, 149-156.
13. B. Liu, M. Zhang, Y. Wang, Z. Chen and K. Yan, J. Alloys Compd., 2021, **852**, 156949.
14. Y. Dong, F. Sun, X. Li, M. Chu, N. Li, X. Li, L. Wang, D. Qu, Y. Dong, Z. Xie, Y. Lin and C. Zhang, J. Electrochem. Soc. 2018, **165**, F1127-F1132.
15. A.A. Lourenço, V.D. Silva, R.B. da Silva, U.C. Silva, C. Chesman, C. Salvador, T.A. Simões, D.A. Macedo and F.F. da Silva, J. Colloid Interface Sci, 2021, **582**, 124-136.

16. M. Dinesh, Y. Haldorai and R.T. Rajendra Kumar, Ceram. Int., 2020, **46**, 28006-28012.

17. S. Adhikari, Y. Kwon and D.-H. Kim, Chem. Eng. J., 2020, **402**, 126192.

18. J. Lu, S. Ji, P. Kannan, H. Wang, X. Wang and R. Wang, J. Alloys Compd., 2002, **844**, 156129.

19. R. Zhang, R. Zhu, Y. Li, Z. Hui, Y. Song, Y. Cheng and J. Lu, Nanoscale, 2002, **12**, 23851-23858.

20. S. Sajjad, C. Wang, X. Wang, T. Ali, T. Qian and C. Yan, Nanotechnology, 2020, **31**, 495404.

21. W. He, F. Wang, D. Jia, Y. Li, L. Liang, J. Zhang, Q. Hao, C. Liu, H. Liu and J. Zhao, Nanoscale, 2020, **12**, 24244-24250.

22. D. Zheng, Z. Jing, Q. Zhao, Y. Kim, P. Li, H. Xu, Z. Li and J. Lin, Chem. Eng. J., 2002, **402**, 125069.

23 G. Janani, S. Yuvaraj, S. Surendran, Y. Chae, Y. Sim, S.-J. Song, W. Park and M.-J. Kim, U. Sim, J. Alloys Compd., 2002, **846**, 156389.

24. H. Han, F. Yi, S. Choi, J. Kim, J. Kwon, K. Park and T. Song, J. Alloys Compd., 2020, **846**, 156350.

25. W. Dai, K. Ren, Y.-a. Zhu, Y. Pan, J. Yu, T. Lu, J. Alloys Compd., 2020, **844**, 156252.